In Vivo Real Time Volumetric Synthetic Aperture Ultrasound Imaging

Bouzari, Hamed; Rasmussen, Morten Fischer; Brandt, Andreas Hjelm; Stuart, Matthias Bo; Nikolov, Svetoslav; Jensen, Jørgen Arendt

Published in:
Proceedings of SPIE

Link to article, DOI:
10.1117/12.2081631

Publication date:
2015

Document Version
Publisher's PDF, also known as Version of record

In Vivo Real Time Volumetric Synthetic Aperture Ultrasound Imaging

Hamed Bouzari[a], Morten Fischer Rasmussen[a], Andreas Hjelm Brandt[b], Matthias Bo Stuart[a], Svetoslav Nikolov[c] and Jørgen Arendt Jensen[a]

[a]Center for Fast Ultrasound Imaging, Department of Electrical Engineering, Technical University of Denmark, Lyngby, Denmark
[b]Department of Radiology, Copenhagen University Hospital, Copenhagen, Denmark
[c]BK Medical ApS, Herlev, Denmark

ABSTRACT

Synthetic aperture (SA) imaging can be used to achieve real-time volumetric ultrasound imaging using 2-D array transducers. The sensitivity of SA imaging is improved by maximizing the acoustic output, but one must consider the limitations of an ultrasound system, both technical and biological. This paper investigates the *in vivo* applicability and sensitivity of volumetric SA imaging. Utilizing the transmit events to generate a set of virtual point sources, a frame rate of 25 Hz for a $90° \times 90°$ field-of-view was achieved. data were obtained using a 3.5 MHz 32×32 elements 2-D phased array transducer connected to the experimental scanner (SARUS). Proper scaling is applied to the excitation signal such that intensity levels are in compliance with the U.S. Food and Drug Administration regulations for *in vivo* ultrasound imaging. The measured Mechanical Index and spatial-peak-temporal-average intensity for parallel beamforming (PB) are 0.83 and 377.5 mW/cm^2, and for SA are 0.48 and 329.5 mW/cm^2. A human kidney was volumetrically imaged with SA and PB techniques simultaneously. Two radiologists for evaluation of the volumetric SA were consulted by means of a questionnaire on the level of details perceivable in the beamformed images. The comparison was against PB based on the *in vivo* data. The feedback from the domain experts indicates that volumetric SA images internal body structures with a better contrast resolution compared to PB at all positions in the entire imaged volume. Furthermore, the autocovariance of a homogeneous area in the *in vivo* SA data, had 23.5% smaller width at the half of its maximum value compared to PB.

Keywords: Real-time volumetric ultrasound imaging, 2-D phased array transducer, synthetic aperture (SA)

1. INTRODUCTION

Volumetric ultrasound enables imaging of the whole volume in one acquisition similar to x-ray computed tomography (x-ray CT) and magnetic resonance imaging (MRI). In conventional 2-D ultrasound imaging, it is required to wait for the propagation of the ultrasound pulse back and forth in the body for each single image line. In volumetric imaging on the other hand, the number of image lines is squared, and hence a quadratic reduction on the achievable frame rate is imposed. Imaging the complex kinematics of organs such as the beating heart requires an increased frame rate, which is far from achievable on large imaging volumes using the conventional approach. Indeed, considering the speed of sound in biological tissues to be around 1540 m/s, about 155 µs are required to acquire a single image line with a 14 cm depth. This is approximately 6400 lines per second which may be used to form a volume of 80×80 image lines, in every second. Von Ramm and Smith[1,2] introduced the first true volumetric ultrasound system, which allowed real-time 3-D scanning at acceptable volume rates. The system applied a parallel beamforming (PB) technique that permitted the formation of a plurality of adjacent lines surrounding the transmit beam direction. To achieve higher volume rates, i.e., higher temporal resolution, broadened transmit beams can be used to illuminate the desired field-of-view resulting in a reduced number of emissions.[3] However, reverberations and aberrations of the ultrasonic wave fronts caused by fatty subcutaneous tissues tend to destroy the focusing capabilities of the system in PB.[4]

Send correspondence to H. Bouzari, E-mail: bouzari@elektro.dtu.dk

Medical Imaging 2015: Ultrasonic Imaging and Tomography, edited by Johan G. Bosch, Neb Duric, Proc. of SPIE Vol. 9419, 94190I · © 2015 SPIE
CCC code: 1605-7422/15/$18 · doi: 10.1117/12.2081631

To recover the focusing capability, while using broad illuminations for a higher temporal resolution, it has been proposed to use synthetic aperture (SA) imaging, originally developed for radar detection systems.[5,6] By coherently combining the data acquired from successive and spatially overlapping ultrasound pulse emissions, one may retrospectively recreate a dynamic transmit focus along each line of the final image. The original SA application used single element excitations, but is now applied using virtual point sources[7] generated with small subsets of transducer elements to increase the energy transfered into the tissue and thereby increase the SNR.

Although SA imaging may allow the spatial resolution to be similar or even improved compared to single line focused ultrasound, it does not ensure a good sensitivity in the sense that, neither the SNR, the penetration nor the contrast are ensured to be similar to what is achieved in conventional ultrasound imaging. The sensitivity is directly related to the characteristics of the emitted pulses: 1) the frequency band and focus depth give an indication of how attenuated a pulse will be, 2) the peak intensity is an indicator of the non-linear effects build-up during the propagation, 3) the aperture size and pulse duration describe the amount of energy transmitted. Thus the sensitivity can be improved by maximizing the acoustic output, but the limitations of the ultrasound system, both technical and biological must be considered. A powerful signal generator to drive a big amount of energy through the piezo-electric transducer is required, which may lead to over-heating of the probe surface. Any damage to the tissues caused by cavitational effects or over-heating has to be avoided. In practice, the acoustic output is adjusted such that both the peak and the temporal average intensities remain under given thresholds.

Previously it has been shown that SA can be used to achieve real-time volumetric imaging based on simulation and phantom studies.[8] However, as of today, it has not yet been successfully adapted to *in vivo* volumetric 2-D phased array imaging. Provost et al.,[9] have done volumetric *in vivo* SA measurements, however they did not provide any other ultrasound volumetric imaging method to compare their results with. In this study, the imaging quality of SA is investigated using *in vivo* measurements. Simulations are used to optimize both techniques before comparison and also to ensure the FDA limits. The optimization is done for a channel limited 3-D ultrasound system with 256 active channels.[9]

The structure of the paper is as follows: First, a brief description of the measurement and simulation setups is given. The point spread functions (PSFs) for the PB and SA are studied both based on simulation and measurement data. The intensity measurements for PB and SA are presented. Then *in vivo* results and the qualitative assessments by experts in the field are presented. Finally, the perspectives of the volumetric SA technique are discussed.

2. MEASUREMENT AND SIMULATION SETUPS

The volumetric data were acquired using the 1024 channel experimental ultrasound scanner, SARUS.[10] To estimate the quality of the SA images compared to PB, the subjects were imaged with both techniques simultaneously. The RF-data were beamformed using the beamformation toolbox 3.[11] Table 1 lists the measurement configuration parameters. The centers of all translated transmit apertures for SA are shown with a dot in Fig. 1(left). The cross is the center of the shown active aperture. The receive aperture which is static during all 256 emissions, is illustrated in Fig. 1 (right). As a trade-off between emitted energy and side-lobe performance, the 24 element wide cross array, seen in Fig. 2 (left), is chosen as the transmit aperture.[8] To get a wide receive aperture and thereby a narrow receive beam main-lobe, the cross array is also used in receive. The widest possible array, a cross array along the diagonals, is chosen as receive aperture. Because the receive aperture is too narrow, it is apodized with a Tukey function with a Ψ parameter close to zero value. The receive aperture is shown in Fig. 2 (right). In Fig. 3, a simulated point spread function example of PB and SA is shown, and can be visually inspected and compared. A point target is located at 62 mm depth and 0° azimuth and elevation tilt angle. In the azimuth plane the sidelobes are larger than in the elevation plane. This is due to three inactive rows of elements on the transducer, all orthogonal to the elevation plane. SA and PB appear to have approximately the same main lobe size. Figure 4, shows the measured 3-D point spread function of PB and SA in a water bath imaging a tip of an iron needle facing toward the transducer and parallel to the center line of the transducer (speed of sound in water 1480 m/s). The apparent noise is due to the low SNR of the research scanner. Figure 5 shows the SNR of the research scanner for both SA and PB in a tissue mimicking phantom. The full width at half maximum (FWHM) and the side lobe energy metrics, for the simulated and measured PSF are listed in table 2.

Table 1. Setup configuration

Center frequency	3		MHz
Pitch x	300		µm
Pitch y	300		µm
Number of elements in x	32		-
Number of elements in y	35 (3 inactive rows)		-
	Techniques		
	SA	PB	
Frame rate	25	25	Hz
Pulse repetition frequency	5.133	5.133	kHz
Emissions per frame	256	256	-
Number of active elements	256	256	-
Scan depth (max range)	14	14	cm
Emission cycles	4	4	-
Focus in transmit	-6	60	mm
Sampling frequency	12	12	MHz
Transmit voltage	±100	±100	V
Field-of-view	90°×90°	90°×90°	-
Beamformed lines per emission	64×64	4×4	-

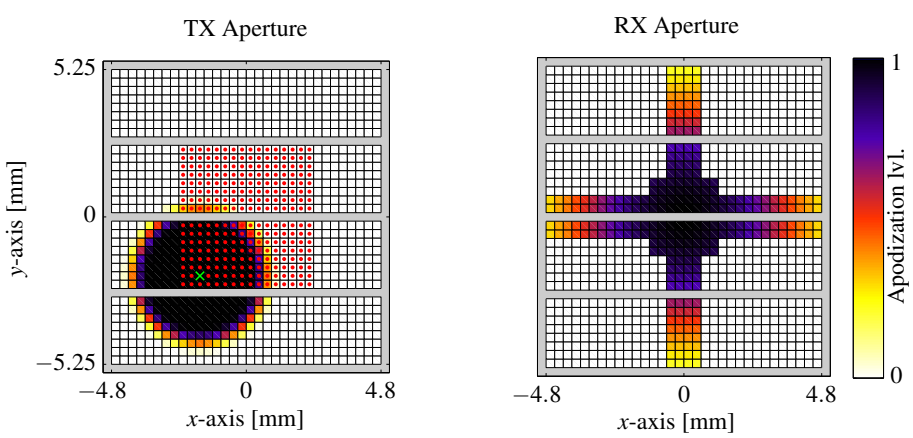

Figure 1. The synthetic aperture imaging transmit and receive apodization implemented on the 32×32 element array. The transmit aperture translates between emission. The center of the shown aperture is illustrated with a green cross. The receive aperture is static during all 256 emissions.

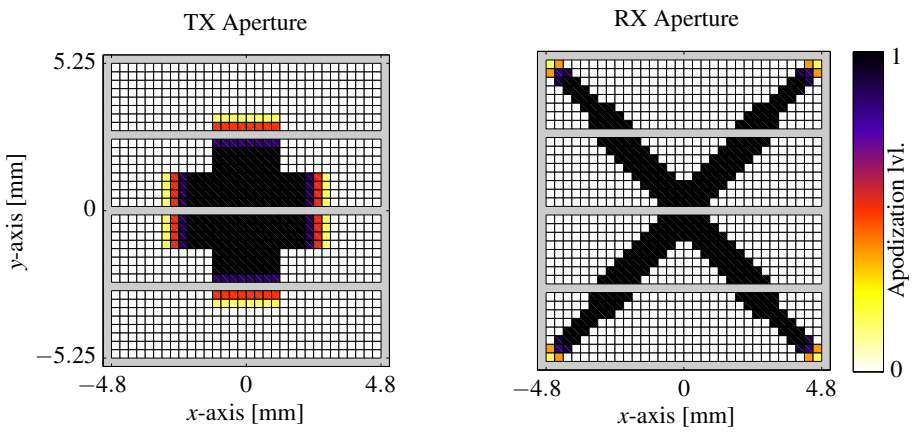

Figure 2. The parallel beamforming transmit and receive apodization implemented on the 32×32 element array. The receive aperture is the widest possible cross array implementable on the 32×32 element array. Both apodizations contain 256 active elements and are used for all 256 emissions.

Table 2. FWHM and side lobe measurements

		SA		PB		
		Simulation	Measurement	Simulation	Measurement	
Cystic resolution (6 dB)[8]		1.55	2.10	2.12	2.67	mm
Cystic resolution (12 dB)[8]		2.22	3.45	3.69	4.68	mm
Cystic resolution (20 dB)[8]		3.47	12.25	7.27	11.77	mm
FWHM (at 62 mm depth)	Axial	0.76	1.14	0.79	1.15	mm
	Azimuth	4.32	4.86	4.78	5.80	mm
	Elevation	4	4.32	4.39	4.34	mm

3. INTENSITY MEASUREMENTS

Before any *in vivo* measurements, the ultrasound imaging technique on the scanner has to fulfill all the requirements regarding the intensity levels and safety limits. Any damage to the tissues caused by cavitational effects or over-heating has to be avoided. In practice, the acoustic output is adjusted such that both the peak and the temporal average intensities remain under given thresholds. As of today, such safety guides are regulated by the the FDA,[12] and take the form of upper limits on given indexes: the mechanical index ($MI \leq 1.9$), the derated spatial-peak-temporal-average intensity ($I_{spta} \leq 720\,\mathrm{mW/cm^2}$ for peripheral vessel, $I_{spta} \leq 430\,\mathrm{mW/cm^2}$ for cardiac), and the derated spatial-peak-pulse-average intensity ($I_{sppa} \leq 190\,\mathrm{mW/cm^2}$).[12] This requires to measure the emitted pressure of the transducer as a function of spatial position. The intensity measurements have been carried out using the experimental ultrasound scanner SARUS and the AIMS III intensity measurement system (Onda Corporation, Sunnyvale, California, USA).[13] The measured MI and I_{spta} before scaling the excitation signal for PB are 0.83 and $377.5\,\mathrm{mW/cm^2}$, and for SA are 0.48 and $329.5\,\mathrm{mW/cm^2}$, accordingly (Table 3).

Table 3. Intensity measurement results

	SA	PB	
Peak MI in water	0.48	0.83	-
Peak MI derated	0.46	0.76	-
Peak I_{spta} in water	329.5	377.5	$\mathrm{mW/cm^2}$
Peak I_{spta} derated	260	312.5	$\mathrm{mW/cm^2}$

4. RESULTS AND DISCUSSION

Cut sections of an *in vivo* volume data of a healthy male's kidney, imaged with SA and PB techniques, are illustrated in Fig. 6. Figure 7 illustrates the magnified areas of the Fig. 6 top row. Two radiologists were consulted for evaluation of volumetric SA by means of a questionnaire and compared SA against PB in terms of the pathological features presented in the *in vivo* data. The PB technique suffers from the block-like artifact. The spatial resolution achieved with SA imaging is dependent on the characteristics of successive transmissions. To achieve higher sensitivity with SA imaging, the energy of each transmitted pulse and also the number of data-sets, which are coherently compounded have to get maximized. But these two constraints imply a trade-off: to maximize the number of combined beams, spatial overlaps between transmitted pulses has to be ensured, and hence use broad beam transmissions where the energy is likely to spread out and the intensity will be reduced. To increase the sensitivity of SA, one may want to increase the energy per pulse by increasing the pulse amplitude or its duration. Increasing the amplitude has an upper limit via MI and I_{spta}. Unfortunately, increasing the pulse duration also will result in a poorer axial resolution. As an alternative, it has been proposed to use linear frequency modulated (FM) excitations combined with match filtering on reception, to increase the energy level without sacrificing the axial resolution.[14] The lateral (elevational) resolution is only defined by the capability of the SA to synthesize a narrow synthetic transmit beam profile.

5. CONCLUSION AND PERSPECTIVES

In this study, a comparison between real-time 3-D synthetic aperture imaging and parallel beamforming using only 256 active channels was made with both Field II simulations and *in vivo* measurements from the experimental ultrasound scanner SARUS. The contrast resolution was improved by synthetic aperture imaging at all positions in the entire imaged volume. The autocovariance of a homogeneous area in the *in vivo* SA data, has 23.5% smaller width compared to PB at the half of its maximum value. Based on the feedbacks from domain experts, the *in vivo* imaging quality of synthetic aperture and parallel beamforming has been investigated. It was shown that using synthetic aperture imaging on a channel limited 3-D ultrasound system can achieve a high image quality at a low cost. Both techniques can volumetrically visualize internal body structures. Visualizing in 3-D gives the clinician a better insight for possible pathology and medical treatments. A novel data visualization tool will become very beneficial in clinical studies, as it is difficult to visualize the ultrasound volume in 3-D.

ACKNOWLEDGMENTS

This work was financially supported by grant 82-2012-4 from the Danish Advanced Technology Foundation and from BK Medical ApS, Herlev, Denmark.

REFERENCES

[1] Smith, S. W., Pavy, H. G., and von Ramm, O. T., "High speed ultrasound volumetric imaging system – Part I: Transducer design and beam steering," *IEEE Trans. Ultrason., Ferroelec., Freq. Contr.* **38**, 100–108 (1991).

[2] von Ramm, O. T., Smith, S. W., and Pavy, H. G., "High speed ultrasound volumetric imaging system – Part II: Parallel processing and image display," *IEEE Trans. Ultrason., Ferroelec., Freq. Contr.* **38**, 109–115 (1991).

[3] Shattuck, D. P., Weinshenker, M. D., Smith, S. W., and von Ramm, O. T., "Explososcan: A parallel processing technique for high speed ultrasound imaging with linear phased arrays," *J. Acoust. Soc. Am.* **75**, 1273–1282 (1984).

[4] Pinton, G., Trahey, G., and Dahl, J., "Erratum: Sources of image degradation in fundamental and harmonic ultrasound imaging: a nonlinear, full-wave, simulation study [apr 11 754-765]," *Ultrasonics, Ferroelectrics and Frequency Control, IEEE Transactions on* **58**, 1272–1283 (June 2011).

[5] Flaherty, J. J., Erikson, K. R., and Lund, V. M., "Synthetic aperture ultrasound imaging systems." United States Patent, US 3,548,642 (1967). United States Patent, US 3,548,642, 1967, Published 22 Dec 1970.

[6] Burckhardt, C. B., Grandchamp, P.-A., and Hoffmann, H., "An experimental 2 MHz synthetic aperture sonar system intended for medical use," *IEEE Trans. Son. Ultrason.* **21**, 1–6 (January 1974).

[7] Nikolov, S. I. and Jensen, J. A., "Virtual ultrasound sources in high-resolution ultrasound imaging," in [*Proc. SPIE - Progress in biomedical optics and imaging*], **3**, 395–405 (2002).

[8] Rasmussen, M. F. and Jensen, J. A., "Comparison of 3-D synthetic aperture phased array ultrasound imaging with parallel beamforming," *IEEE Trans. Ultrason., Ferroelec., Freq. Contr.* **61**(10), 1638–1650 (2014).

[9] Provost, J., Papadacci, C., Arango, J. E., Imbault, M., Fink, M., Gennisson, J. L., Tanter, M., and Pernot, M., "3d ultrafast ultrasound imaging in vivo," *Physics in Medicine and Biology* **59**(19), L1–L13 (2014).

[10] Jensen, J. A., Holten-Lund, H., Nilsson, R. T., Hansen, M., Larsen, U. D., Domsten, R. P., Tomov, B. G., Stuart, M. B., Nikolov, S. I., Pihl, M. J., Du, Y., Rasmussen, J. H., and Rasmussen, M. F., "SARUS: A synthetic aperture real-time ultrasound system," *IEEE Trans. Ultrason., Ferroelec., Freq. Contr.* **60**(9), 1838–1852 (2013).

[11] Hansen, J. M., Hemmsen, M. C., and Jensen, J. A., "An object-oriented multi-threaded software beamformation toolbox," in [*Proc. SPIE Med. Imag.*], **7968**, 79680Y 1–9 (March 2011).

[12] FDA, "Information for manufacturers seeking marketing clearance of diagnostic ultrasound systems and transducers," tech. rep., Center for Devices and Radiological Health, United States Food and Drug Administration (2008).

[13] Jensen, J. A., Rasmussen, M. F., Stuart, M. B., and Tomov, B. G., "Simulation and efficient measurements of intensities for complex imaging sequences," in [*Proc. IEEE Ultrason. Symp.*], 1164–1167, IEEE (2014).

[14] Misaridis, T. and Jensen, J. A., "Use of modulated excitation signals in ultrasound, Part III: High frame rate imaging," *IEEE Trans. Ultrason., Ferroelec., Freq. Contr.* , 220–230 (2005).

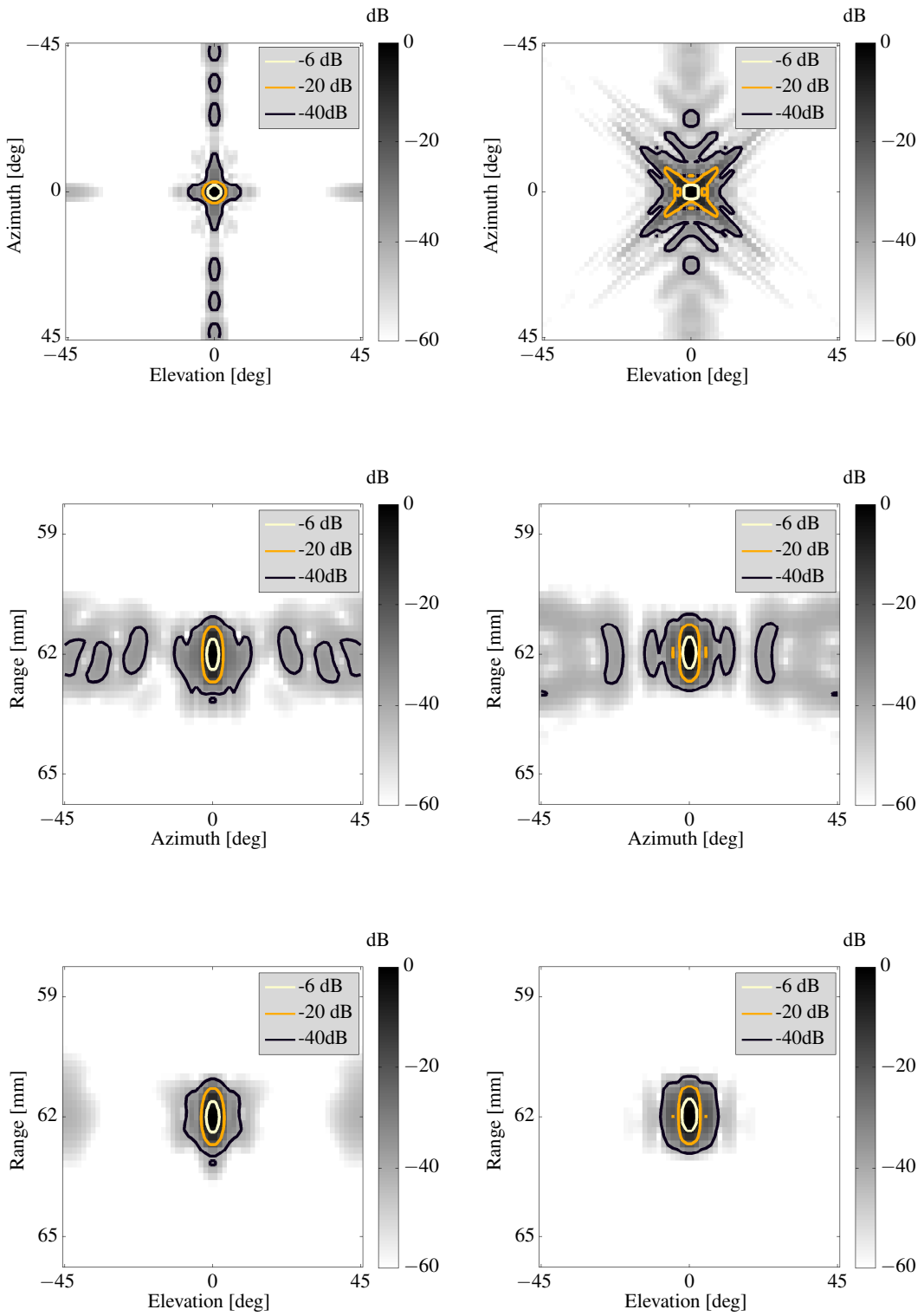

Figure 3. PB and SA simulated 3-D point spread function sliced into three 2-D planes. The point spread functions are observed at 62 mm depth and 0° azimuth and elevation tilt angle. The left column is SA and the right column is PB.

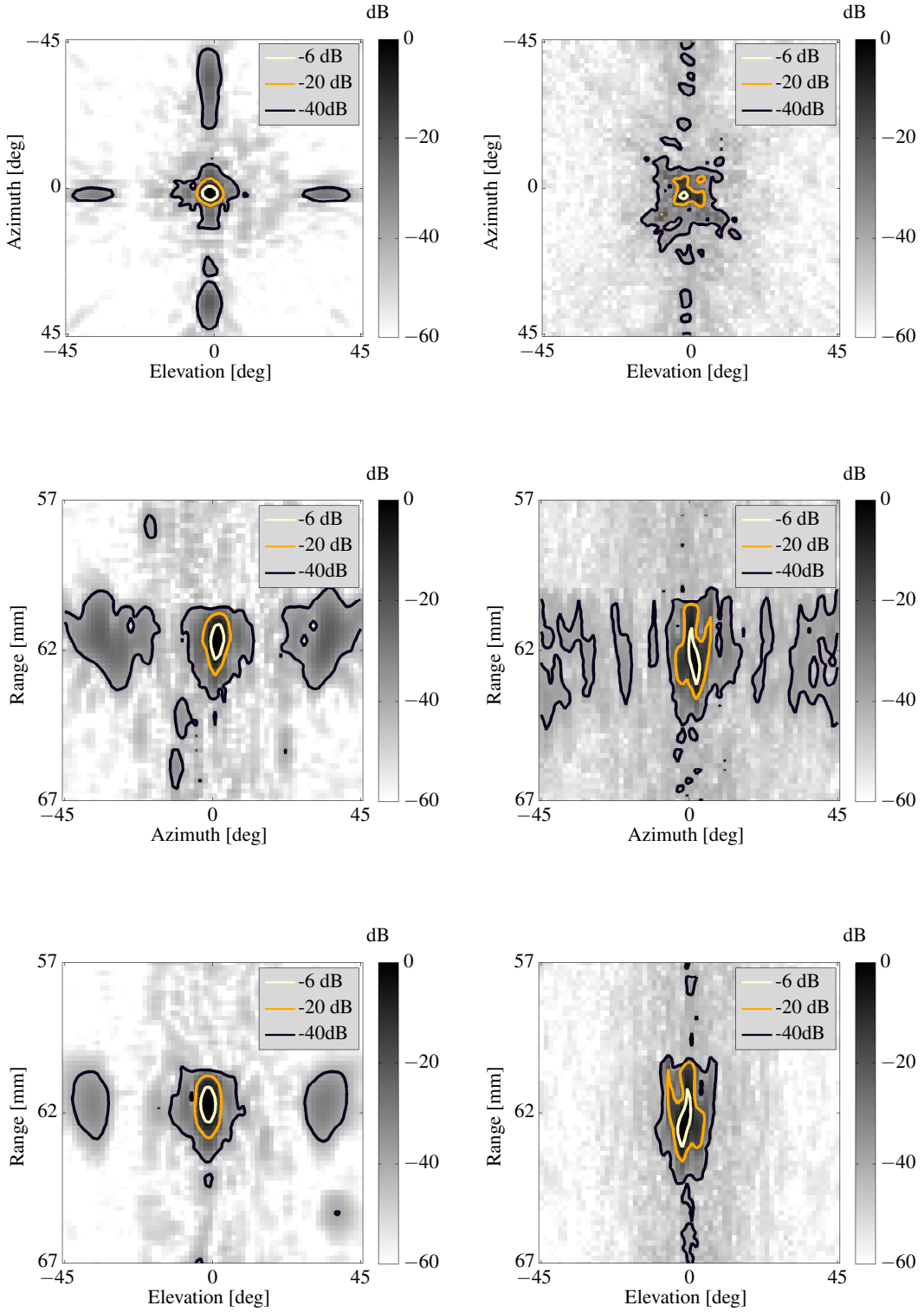

Figure 4. PB and SA measured 3-D point spread function sliced into three 2-D planes. The point spread functions are observed at 62 mm depth and 0° azimuth and elevation tilt angle. The left column is SA and the right column is PB.

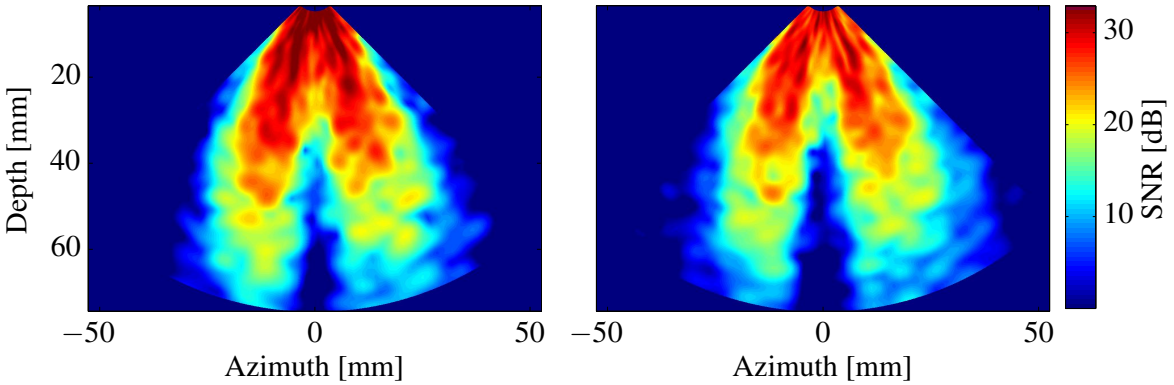

Figure 5. The SNR of the research scanner for both SA (left) and PB (right) imaging methods in a tissue mimicking phantom.

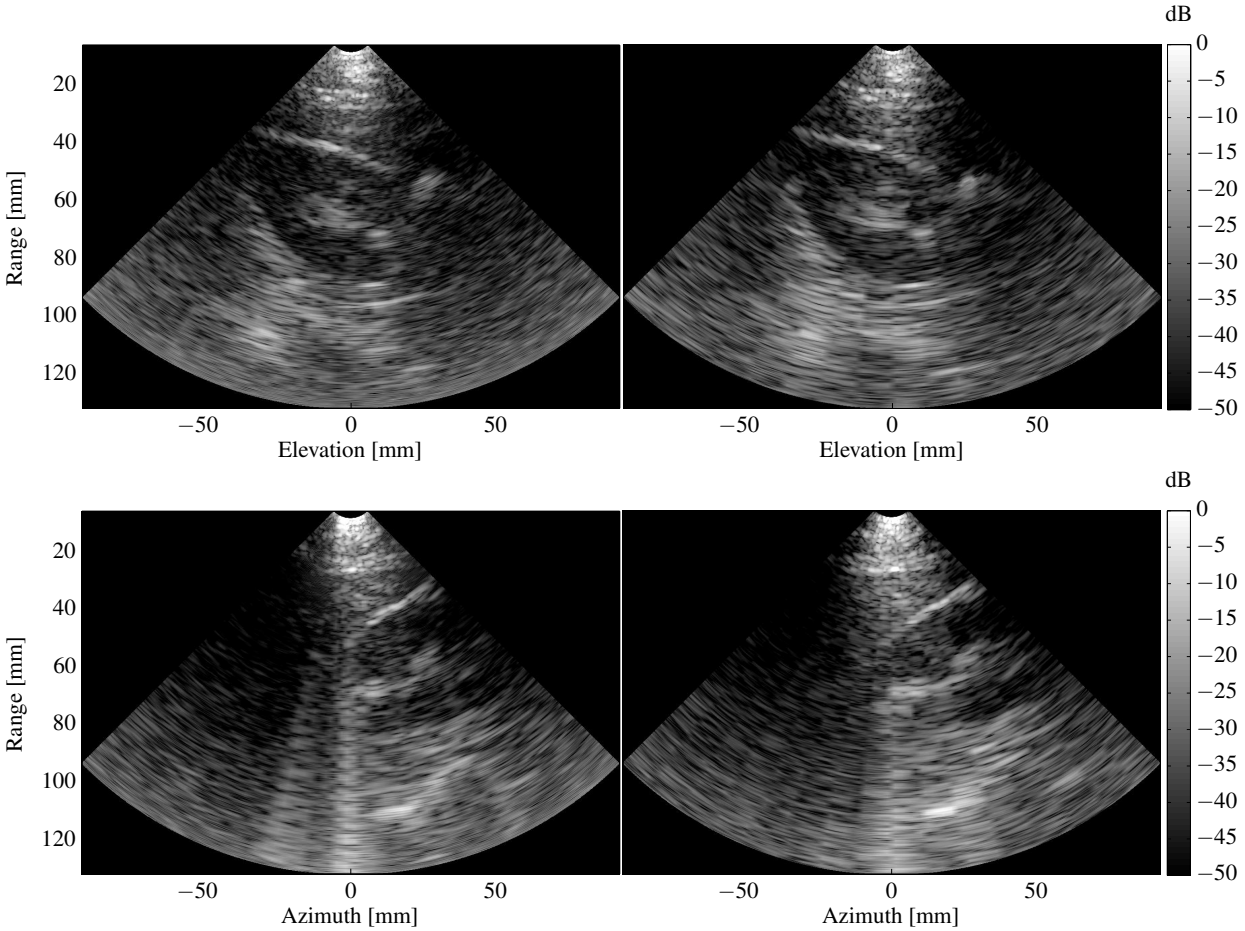

Figure 6. Cut sections of an *in vivo* volume of a human kidney imaged with PB and SA techniques. The left column is SA and the right column is PB.

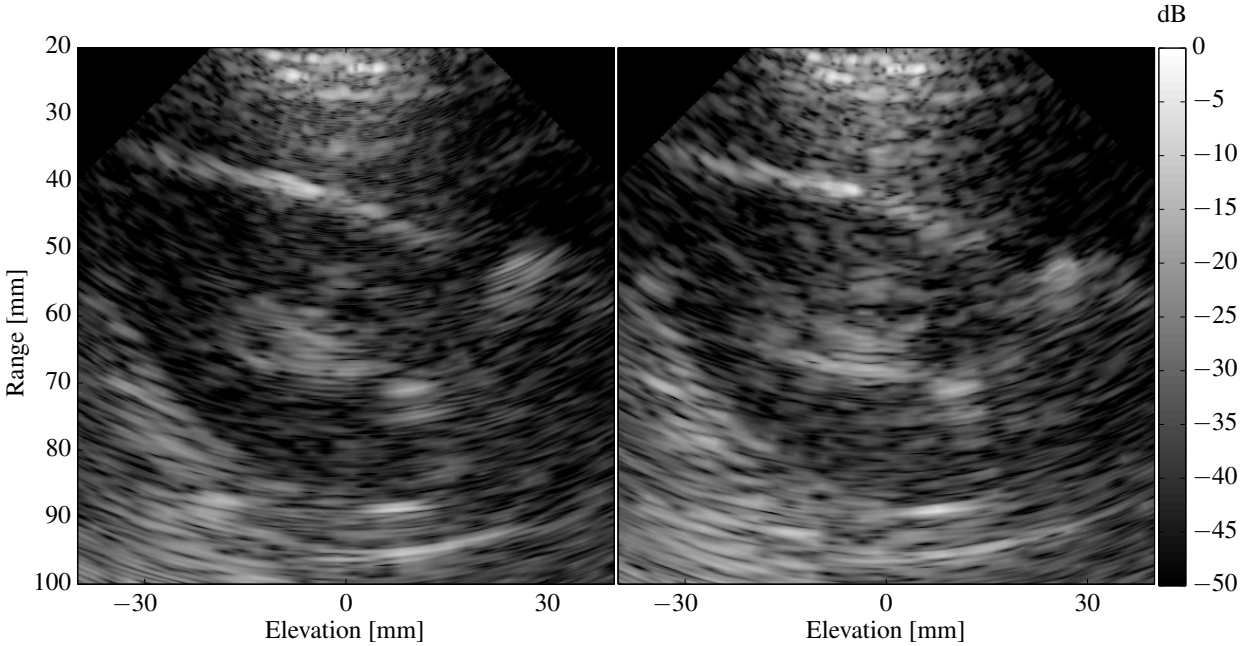

Figure 7. The magnified areas of the *in vivo* image of a human kidney imaged with PB and SA techniques shown in top row of Fig. 6. The left one is SA and the right one is PB.